

CHAPTER 42

Reevaluating Late-Pleistocene and Holocene Active Faults in the Tahoe Basin, California-Nevada

Graham Kent

Nevada Seismological Laboratory, University of Nevada, Reno, Reno, Nevada 89557-0174, USA

Gretchen Schmauder

Nevada Seismological Laboratory, University of Nevada, Reno, Reno, Nevada 89557-0174, USA Now at: Geometrics, 2190 Fortune Drive, San Jose, California 95131, USA

Jillian Maloney

Department of Geological Sciences, San Diego State University, San Diego, California 92018, USA

Neal Driscoll

Scripps Institution of Oceanography, University of California, San Diego, 9500 Gilman Drive, La Jolla, California 92093, USA

Annie Kell

Nevada Seismological Laboratory, University of Nevada, Reno, Reno, Nevada 89557-0174, USA

Ken Smith

Nevada Seismological Laboratory, University of Nevada, Reno, Reno, Nevada 89557-0174, USA

Rob Baskin

U.S. Geological Survey, West Valley City, Utah 84119, USA

Gordon Seitz

California Geological Survey, 345 Middlefield Road, MS 520, Menlo Park, California 94025, USA

ABSTRACT

A reevaluation of active faulting across the Tahoe basin was conducted using a combination of airborne LiDAR (Light Detection and Ranging) imagery, high-resolution seismic CHIRP (acoustic variant, compressed high intensity radar pulse) profiles, and multibeam bathymetric mapping. In August 2010, the Tahoe Regional Planning Agency (TRPA) collected 941 square kilometers of airborne LiDAR data in the Tahoe basin. These data have a density of 11.82 points per square meter, with approximately 2 points per square meter striking

the bare earth; the vertical accuracy of this dataset approaches 3.5 centimeters. The combined lateral and vertical resolution has refined the landward identification of fault scarps associated with the three major active fault zones in the Tahoe basin: the West Tahoe–Dollar Point fault, Stateline–North Tahoe fault, and Incline Village fault. By using the airborne LiDAR dataset, we were able to identify previously unmapped fault segments throughout the Tahoe basin, which heretofore were difficult to trace due to thick vegetation covering rugged alpine terrain. To refine fault locations beneath Lake Tahoe, Fallen Leaf Lake and Cascade Lake,

we acquired additional seismic CHIRP imagery using an Edgetech Subscan system. By combining CHIRP and LiDAR imagery, together with new multibeam bathymetry collected in Fallen Leaf Lake (Maloney et al., 2013), we were able to identify previously unknown fault segments, rectify those which had been misplaced, and document better continuity along individual fault systems. Additionally, we have correlated the timing of debris flow and turbidite deposits in Lake Tahoe near the Stateline–North Tahoe fault (Crystal Bay escarpment) and integrated this information into the comprehensive history of Holocene fault rupture in the basin. The new indirect evidence of ground shaking as recorded in shallow lacustrine stratigraphy suggests the potential for synchronicity of rupture between West Tahoe–Dollar Point and Stateline–North Tahoe faults. Through integration of complementary geophysical datasets, we have developed a much-improved model of fault architecture and timing within the Tahoe basin, which presents a much simpler mode of normal faulting in this basin in contrast to earlier investigations by Schweickert et al. (2004) and Howle et al. (2012) that interpreted a much greater density/complexity of faults. Our updated fault map provides a better understanding of the tectonics of the basin, and will help constrain future earthquake magnitudes and associated seismic hazards, such as ground ruptures and tsunamis.

Introduction and Rationale

Lake Tahoe occupies the westernmost basin within the trans-tensional Walker Lane deformation belt that abuts the eastern edge of the Sierra Nevada microplate (Unruh et al., 2003; Schweickert et al., 2004; Kent et al., 2005; Dingler et al., 2009; Brothers et al., 2009; Maloney et al., 2013; Busby, 2013). New geodetic surveys suggest that approximately 7 mm/yr, or about 15 percent of the total plate motion between the Pacific plate and the North American plate, is accommodated along this boundary near Lake Tahoe (Bormann, 2013); the majority of slip in this region of the northern Walker Lane is accommodated through dextral shear, although the exact distribution of this motion (e.g., strike-slip versus block rotation) remains

unclear (Cashman and Fontaine, 2000; Wesnousky et al., 2012). Geodetic data suggest that the Tahoe basin accommodates equal amounts of extension (on mapped normal faults) and right-lateral shear (Hammond et al., 2011), but compelling evidence for the strike-slip component is sparse. The gradual opening-to-the-north geometry of the Tahoe basin, however, may suggest some form of left-lateral accommodation at the northern end of the basin.

Prior to acquisition of a basin-wide LiDAR dataset, mapping faults in the Tahoe basin was hampered not only by the presence of glacial deposits, but also by dense brush and forests, seasonal snow, and by the lake itself. Lindgren (1911) first recognized that the basin-bounding faults extend north into the Truckee basin. Additional work by Blackwelder (1933) and Birkeland (1963) continued to study the basin and its associated faults. Hyne et al. (1972) performed the earliest marine seismic studies in Lake Tahoe, providing the first views of fault architecture at the bottom of the lake, and Gardner et al. (2000) provided further evidence of a right-stepping, en-echelon normal fault system through a comprehensive multibeam survey of Lake Tahoe. Schweickert et al. (2004) published the first comprehensive fault map of the entire basin showing numerous and complex faults. The faults were particularly abundant near the mapped West Tahoe–Dollar Point fault (WTDPF) on the west side of the lake, as well as in the northern portion of the lake, coinciding with the Stateline–North Tahoe fault (SLNTF) and Incline Village fault (IVF). In contrast, faults mapped within lacustrine sediments using a sub-bottom CHIRP profiler in Lake Tahoe, Cascade Lake and Fallen Leaf Lake (Kent et al., 2005; Dingler et al., 2009; Brother et al., 2009; Maloney et al., 2013) presented a simpler pattern. These lake-based maps, while clearly identifying the WTDPF, SLNTF and IVF, did not exhibit the same complexity or density of secondary faults (Fig. 1), as reported in the onshore fault maps by Schweickert et al. (2004) and Howle et al. (2012). These observations raise the following question: why is faulting observed on land so much more complex than that imaged in the lake? In principle, mapping faults and associated structures is rather straightforward in a lacustrine environment

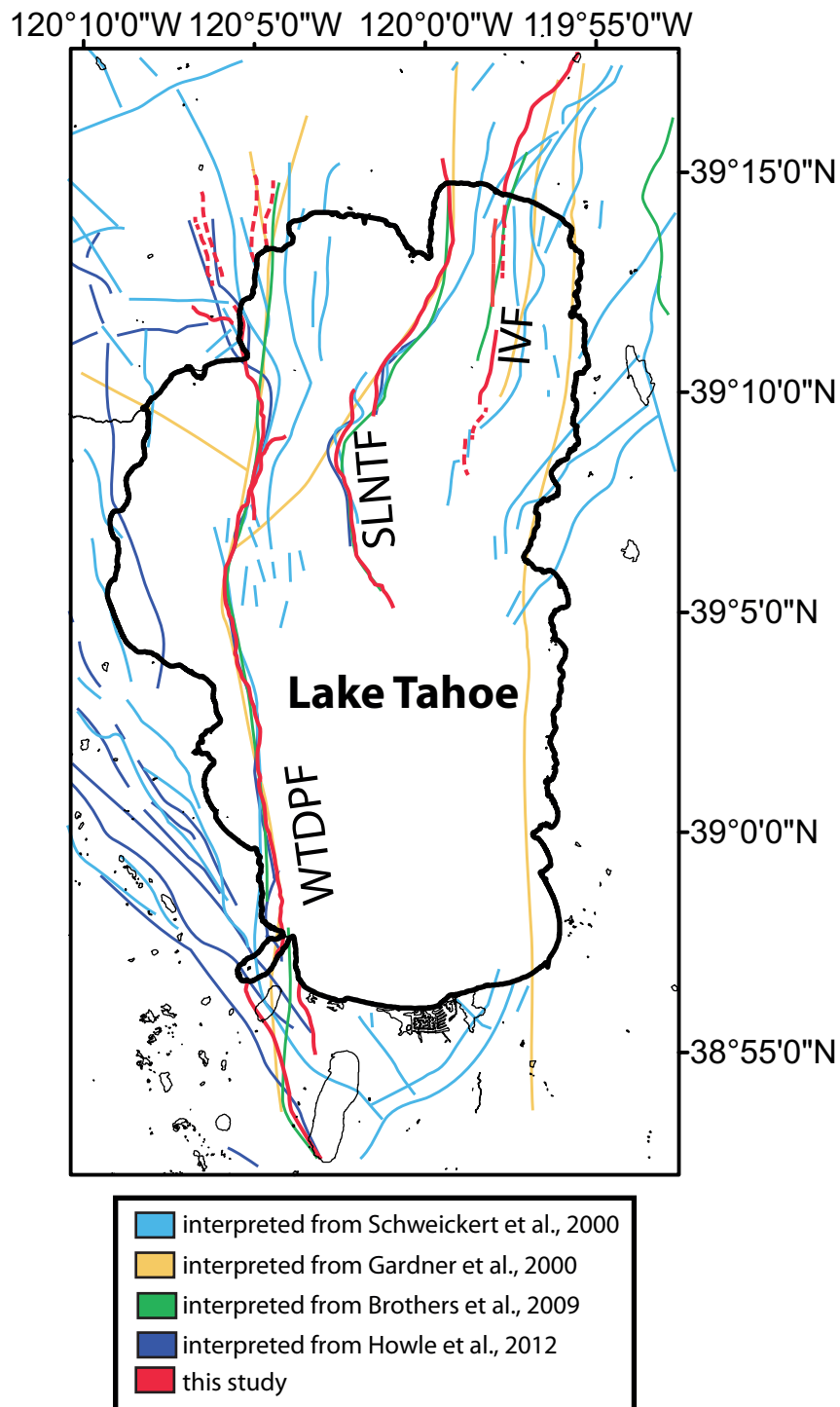


Figure 1. A schematic diagram of fault density from various studies in the Lake Tahoe basin. The results from our study highlight a simple right-stepping, en-echelon normal fault system (red) that is in stark contrast to several previous fault studies (blue and cyan), where fault densities are dramatically different. Also, previous faults such as the East Tahoe fault (gold, eastern shoreline) have been removed from our current map as no signature in either LiDAR imagery or seismic profiling was found. West Tahoe-Dollar Point fault (WTDPF), Stateline-North Tahoe fault (SLNTF) and Incline Village fault (IVF) are shown.

such as the Tahoe basin; is there a geologic reason for this dichotomy? Perhaps mapping of faults on land provides a greater integration of time, thus being more sensitive to recording motion on faults with diminished slip-rates relative to the large basin bounding faults? Tahoe and Tioga deposits and landforms (Birkeland, 1963) provide excellent markers for late Pleistocene and Holocene fault movement, but in many cases may erase or inhibit mapping of older histories of rupture on land. Lastly, the mismatch between fault systems on land and in the lakes may simply be a misinterpretation in the geologic processes that shape the basin, resulting in incongruous maps. To this end, a comprehensive geophysical approach described below has been employed in both environments to attempt to resolve this issue and provide an updated fault map of late Pleistocene and Holocene rupture in the Tahoe basin, and test whether there is an obvious component of right-lateral slip on these faults, or newly discovered faults owing to the new capabilities of this LiDAR dataset.

Methods:

In 2010, the Tahoe Regional Planning Agency (TRPA) commissioned Watershed Sciences to fly an airborne LiDAR survey of the Tahoe basin (Fig. 2; Figs. 3-6). Our group was involved with data specification, contractor selection and data quality control. Although the TRPA commissioned the survey for land-use planning purposes, due to the high pulse density of the data, active fault scarps across the basin could be easily identified. The flight paths and LiDAR instrumentation were designed to achieve a pulse density ≥ 8 pulses per square meter. Over 11 pulses per square meter were shot with approximately 2 strikes per square meter hitting the bare earth. Processing the resulting point cloud supported a 0.5-meter pixel resolution bare earth model of the Tahoe basin (Watershed Sciences, 2010), although data were resampled to 1 m grids. The raw LiDAR data were processed to remove the vegetation signal, resulting in a bare earth model suitable for geologic mapping purposes; after identifying faults scarps on the processed bare earth data, each trace was then verified through a field investigation. This process

was further aided by fault exploration within the QPS *Fledermaus* 3-D interpretational environment (<http://www.qps.nl/display/fledermaus>) that allows active slope shading of hillsides, and integration with other datasets, including multibeam bathymetric maps and seismic CHIRP profiles.

Beginning the in summer of 1999, Scripps Institution of Oceanography and the University of Nevada, Reno and have undertaken several CHIRP sonar campaigns (1999, 2000, 2002, 2006 and 2011) to investigate and then refine the architecture of submerged faults that exist beneath Lake Tahoe, Emerald Bay, Fallen Leaf Lake, and Cascade Lake (Kent et al., 2005; Dingler et al. 2009; Brothers et al., 2009; Maloney et al., 2013). The CHIRP sonar has an effective penetration of approximately 50-70 meters into the lake bottom sediments with sub-meter vertical accuracy. The new CHIRP data (2011) presented in this manuscript used either 0.7-3 kHz or 1-15 kHz pulses, with a 30 ms swept pulse. Observations made from the CHIRP profiles include fault locations, fault offset, and the extent of landslide/debris deposits.

Observations:

West Tahoe–Dollar Point fault

The West Tahoe-Dollar Point fault (WTDPF) bounds the western side of the Tahoe basin, starting in the south near Echo Summit, where it strikes northwestward through Fallen Leaf Lake and Cascade Lake, then steps north into Lake Tahoe near Emerald Bay, where it bounds the steep western escarpment offshore of Rubicon. The WTDPF then traverses through McKinney Bay, reemerging onshore near Dollar Point. For clarity in discussing the WTDPF, it has been divided it into three geometric segments. These are the Fallen Leaf Lake segment (FLS), the Rubicon segment (RS), and the Dollar Point segment (DPS) (Fig. 2).

Fallen Leaf Segment

LiDAR imagery of the FLS of the WTDPF is shown in a 3-D perspective between Echo Summit and Fallen Leaf Lake (Fig. 7). As imaged in Figures 3&7, the fault scarp is clearly visible south of Highway 50, where it dies out towards Christmas Valley. It continues northward, where

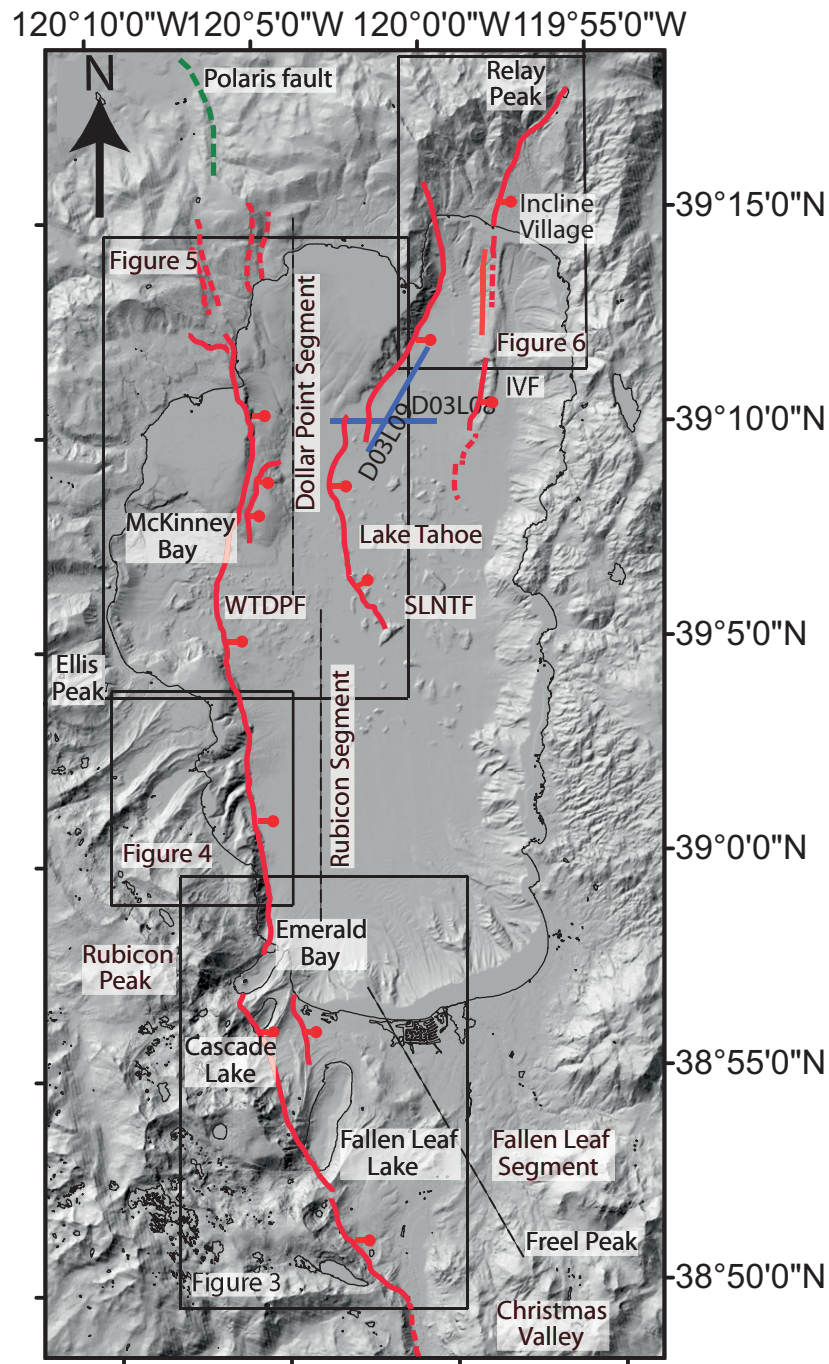


Figure 2. Regional map of the Lake Tahoe basin that highlights the comprehensive LiDAR coverage of the entire basin, along with the location of the observed faults (red) and CHIRP profiles (blue) discussed in this paper. West Tahoe–Dollar Point fault (WTDPF), Stateline–North Tahoe fault (SLNTF), and Incline Village fault (IVF) are shown. Segmentation of the WTDPF is also highlighted: Fallen Leaf segment, Rubicon segment and Dollar Point segment. Debris from the McKinney Bay slide is evident as the blocky features located near the middle of the lake and are shown in more detail in Figure 5. The boxes outlined on the map show the locations of detailed imagery (Figs. 3-6). Approximate location of the Polaris fault indicated by dashed green line. Locations of several landmarks are also highlighted on this map.

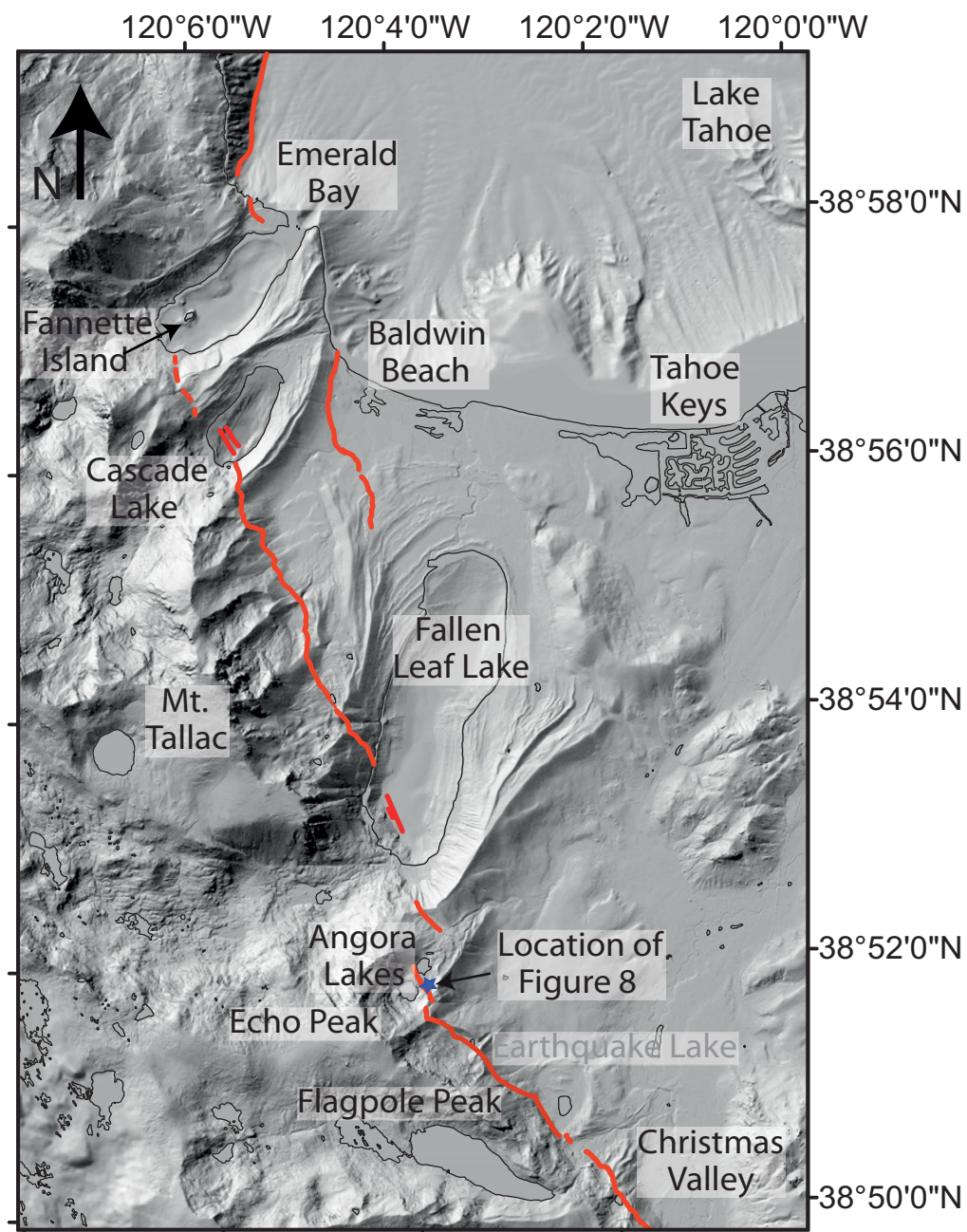


Figure 3. Detailed map showing the Fallen Leaf Lake segment of the West Tahoe–Dollar Point fault in the southwestern portion of the basin. The strands of the WTDPF are shown in red. Additional landmarks are noted.

it crosses Highway 50 and then skirts along the base of Flagpole Peak before climbing the side of Echo Peak. It then traverses across an ephemeral lake (also known as Earthquake Lake), and cuts between the Upper and Lower Angora Lakes before stepping into Fallen Leaf Lake. Previous work by

Brothers et al. (2009) inferred that the FLS fault trace must be topographically lower (following a straight line) and lie in the valley at the base of Flagpole Peak, as more obvious sections near Echo Summit and Angora Lakes were already identified in their study. Our analysis of the new LiDAR data

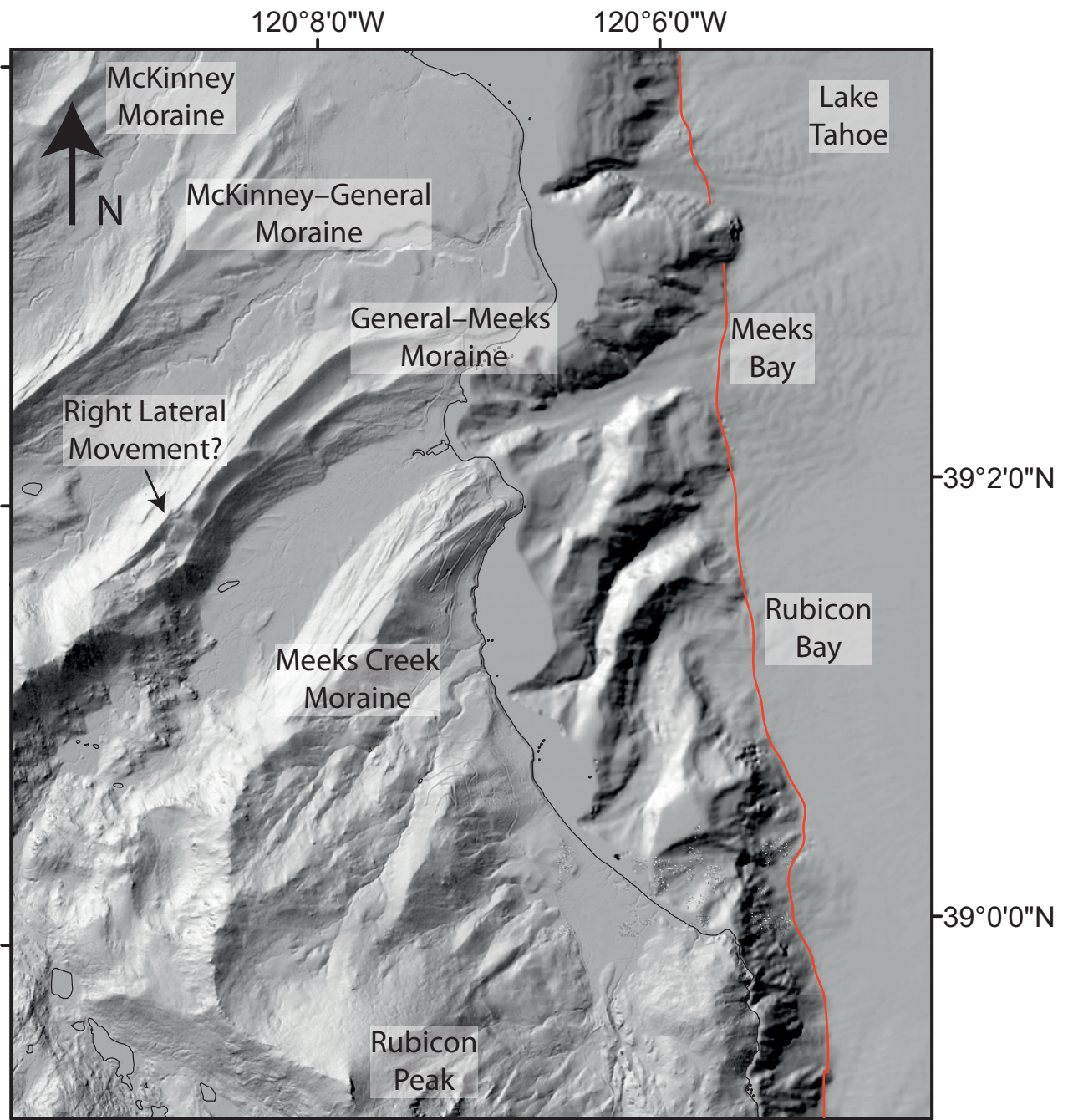


Figure 4. Detailed map of the Rubicon segment of the West Tahoe–Dollar Point fault (shown in red). Along this section, a steep wall formed by this down-to-the-east normal fault characterizes the western edge of the lake. Locations of moraines near Meeks Bay are highlighted, along with location of potential right-lateral slip offsetting the recessional moraine.

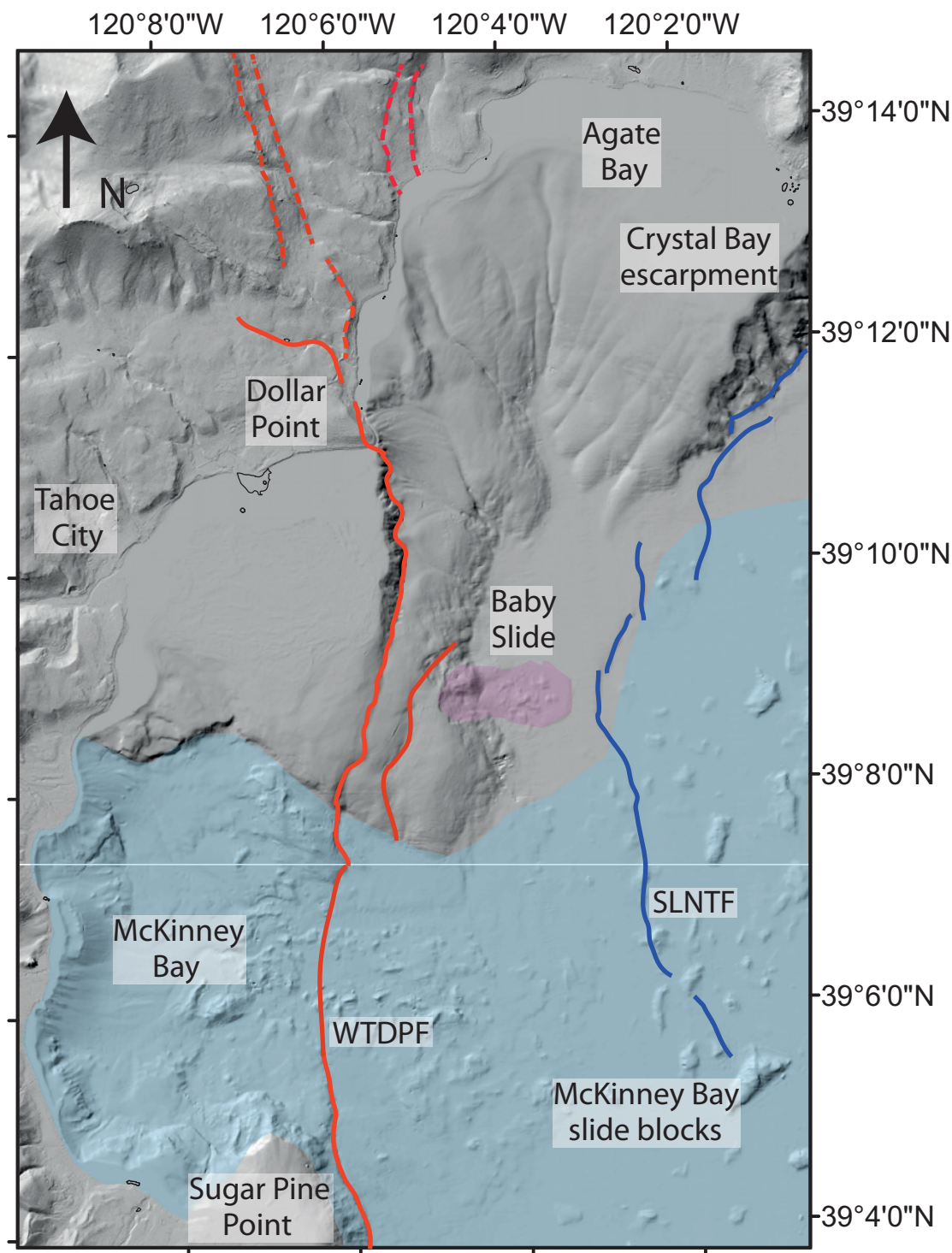


Figure 5. Detailed map of the Dollar Point segment of the West Tahoe–Dollar Point fault (shown in red). The West Tahoe–Dollar Point fault is seen cutting through McKinney Bay and continuing across the Tahoe shelf, before trending north-northwest and back onto land. The blue lines represent the Stateline–North Tahoe fault from its observed southern terminus as it trends northward. The development of a scarp can be observed in the northerly trending portion of this fault. The extent of the McKinney Bay landslide (<60,000 years before present; Kent et al., 2005) is shown outlined in light blue shading. Large slide blocks are shown on the east side of this figure. The Baby Slide, as described in Smith et al. (2013), is shown in pink. West Tahoe–Dollar Point fault (WTDPF) and Stateline–North Tahoe fault (SLNTF) are shown.

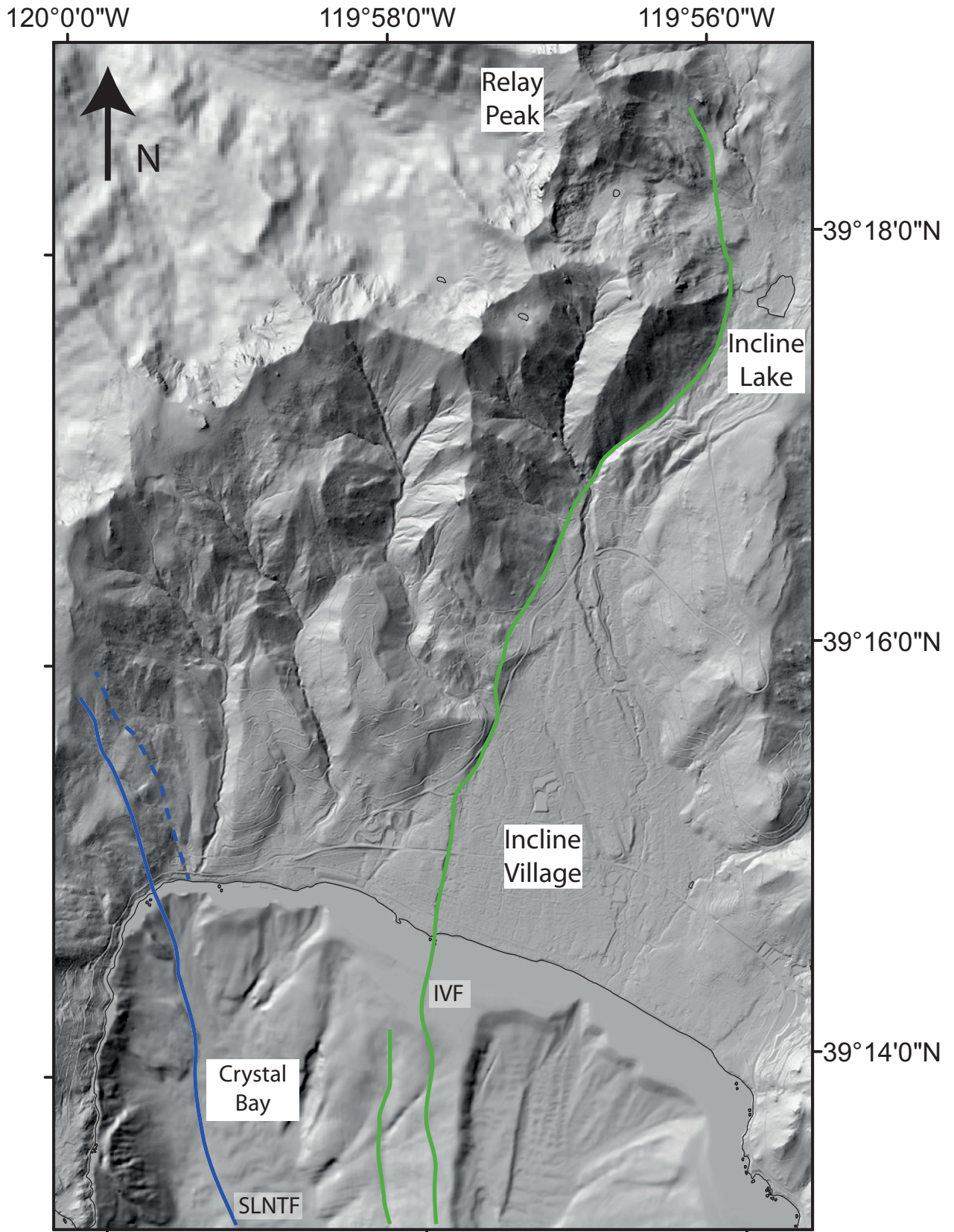


Figure 6. Detailed image of the northern portion of the Tahoe basin, which highlights the Incline Village fault (olive green) and northern terminus of the Stateline–North Tahoe fault. Locations of Relay Peak and Crystal Bay are also shown. Stateline–North Tahoe fault (SLNTF) and Incline Village fault (IVF) are shown.

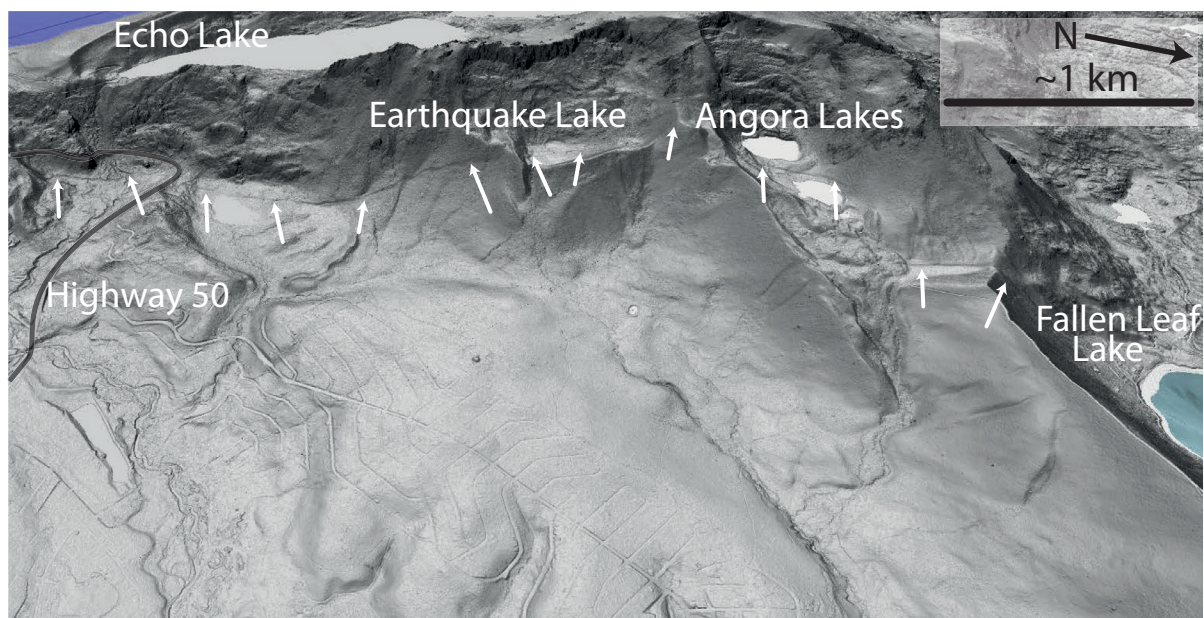


Figure 7. A slope-shade bare earth LiDAR image of the southern extent of the West Tahoe–Dollar Point fault from its southern terminus in Christmas Valley through to its descent into Fallen Leaf Lake. The scarp is clearly visible in the LiDAR imagery near Echo Summit, where it then trends upward along the mountain front before cutting between the Upper and Lower Angora Lakes.

indicates that portions of this fault are not confined to the base of the range front, but instead locally climb upslope. Though previous movement on the fault is undoubtedly responsible for Christmas Valley at the base of Flagpole Peak, the most recent movement appears to be encroaching westward, as is evidenced by fault scarps observed upslope. It should also be noted that there are several large stepovers along the fault, including a nearly one-half kilometer right step near Angora Lakes.

A photo of the fault scarp as observed on the ground between the Upper and Lower Angora Lakes is shown in Figure 8. At this location, breaks in slope across the fault scarp may suggest multiple (potentially two or three) slip events with an offset of approximately two meters per event. There is an obvious temporal component to weathering, as the top of the scarp has more weakly defined scarp faces, suggesting longer exposure to the elements. The top and bottom offset surfaces appear to be related to Tioga-aged glacial outwash mantling a recessional moraine, which resulted in a very flat surface that defines the total throw across the fault scarp with a maximum height of ~6 meters.

North of Angora Lakes, the WTDPF scarp continues through the southern end of Fallen Leaf Lake, where it forms a large escarpment that is imaged in the multibeam sonar bathymetric dataset and vertical CHIRP cross-sections (Maloney et al., 2013; Brothers et al., 2009). Curiously, a second branch of the fault appears to form onshore just northwest of Fallen Leaf Lake and continue towards Baldwin Beach at Lake Tahoe (Figs. 2&3). It is difficult to determine how or if this branch continues south and connects up with the main strand of the fault. The main branch traverses near Mt. Tallac, where it crosses Cascade Lake (Fig. 3&9). The FLS is imaged as two distinct faults in Cascade Lake CHIRP data (Maloney et al., 2013). The main fault trace may continue a bit farther northwest, through a saddle in the moraine, and into Emerald Bay, where there is weak evidence from CHIRP profiling of stratal divergence towards the south (Maloney et al., 2013). However, clear evidence of a scarp in the LiDAR data is lacking between Cascade Lake and Emerald Bay. Maloney et al. (2013) suggests that the fault may continue on the east side of Fanette Island before stepping some 1.5 km towards the precipitous western edge of Lake

Tahoe that defines the RS of the WTDPF. There is weak evidence for fault scarps continuing onshore to the northwest from southern Emerald Bay in the LiDAR data. Landslide scarps are observed approximately four kilometers north of Emerald Bay (Fig. 10). These features exhibit geomorphology typically associated with landslides, such as arcuate head scarps, slump blocks and glide planes.

Rubicon Segment

The RS of the WTDPF is not observed on land, with the exception of a small slice of the fault and corresponding scarp observed on a flat bench near the northern entrance to Emerald Bay, which can be observed in the LiDAR dataset (Figs. 3&10). Continuing north, the fault trace plunges into the lake and follows the steep western wall of Lake Tahoe, which is observed in bathymetric and CHIRP

data. This segment, extending from the mouth of Emerald Bay to the mid-section of McKinney Bay, is characterized by a steep, submerged escarpment, approximately 400 meters in height, and offsets a small fan delta at the base of the steep wall (Fig. 10). The fault scarp terminates abruptly at McKinney Bay, where the lakeshore shifts sharply to the west. This termination is a result of the McKinney Bay slide (Gardner et al., 2000), which has altered the shoreline and reduced the height of the fault-related escarpment. This megaslide (Fig. 5) is thought to be roughly 60 ka in age (Kent et al., 2005). Since this catastrophic event, smaller slides sourced to the west continue to mask the development of a continuous fault scarp (Smith et al., 2013). In the LiDAR data, recent (Holocene or younger) faulting does not appear to offset the onshore moraines between Emerald Bay and McKinney Bay



Figure 8. Photograph showing the Fallen Leaf segment of the West Tahoe–Dollar Point fault scarp, where the fault cuts between the Upper and Lower Angora Lakes. Location of the photograph is shown in Figure 3.

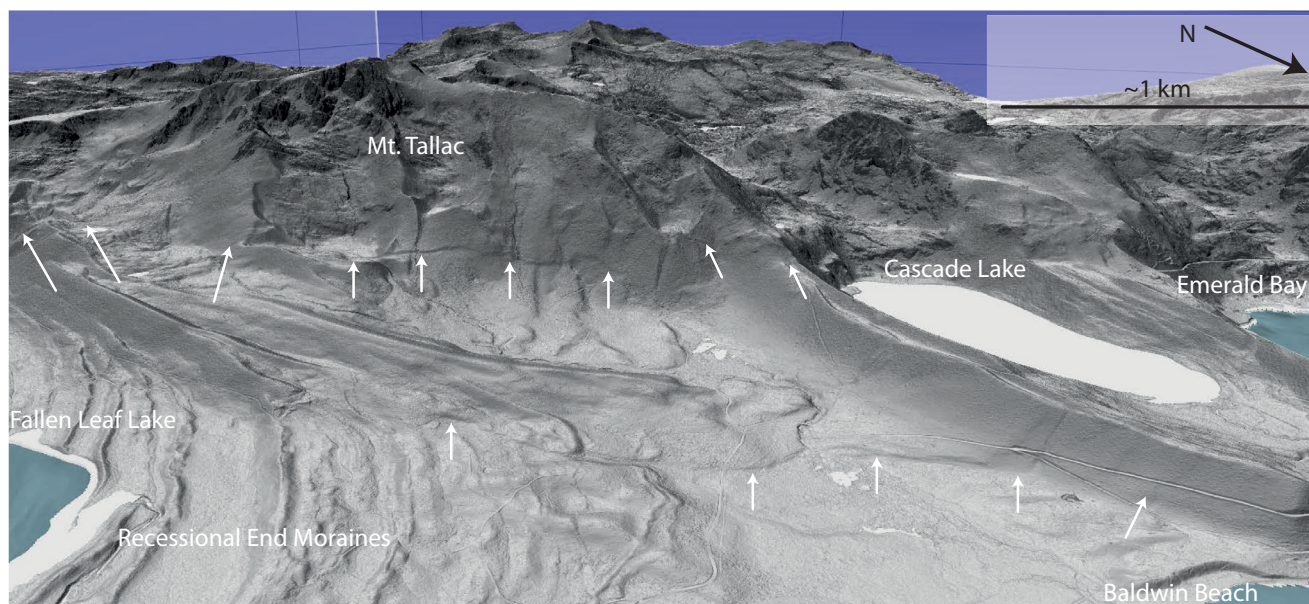


Figure 9. A slope-shade bare earth LiDAR image of the West Tahoe–Dollar Point fault near the vicinity of Mt. Tallac is shown. The fault scarp is clearly visible in the LiDAR imagery, where it cuts along the face of Mt. Tallac and then crosses near the southwestern shore of Cascade Lake. North of Fallen Leaf Lake, the fault also plays to the east and forms a second, fairly continuous trace toward Baldwin Beach on the shores of Lake Tahoe.

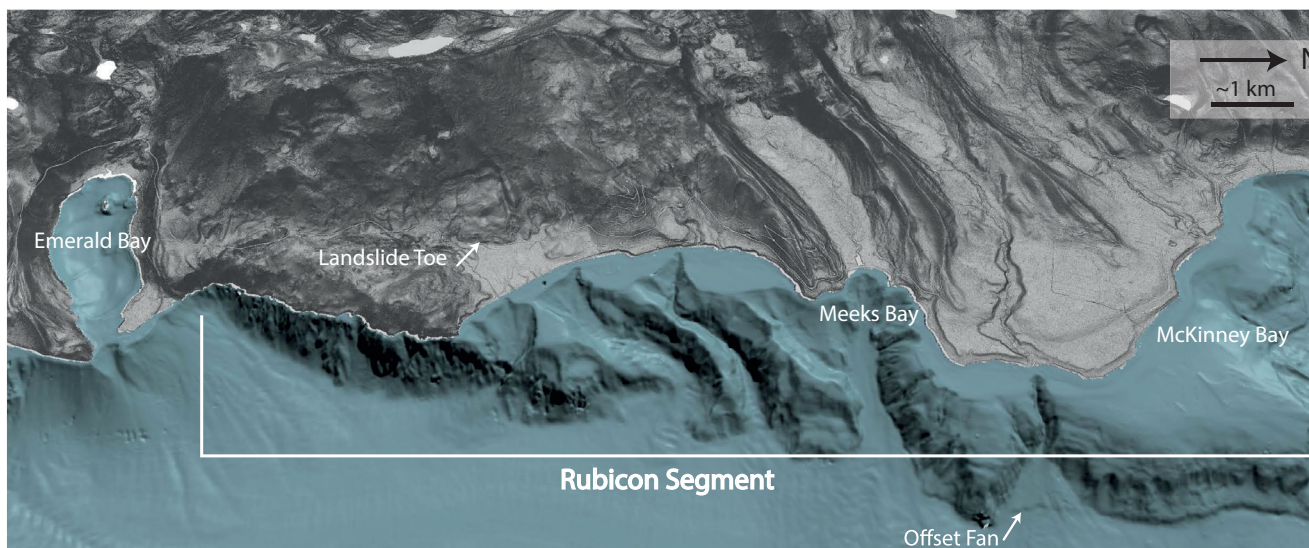


Figure 10. A slope-shade bare earth LiDAR model of the Tahoe- and Tioga-aged moraines south of McKinney Bay merged with swath bathymetry data from Lake Tahoe. Recent (latest Pleistocene or younger) faulting does not appear evident across these moraines. Older bedrock faulting may be present beneath these glacial deposits, though faulting of the character observed in this study along the southern portion of the West Tahoe–Dollar Point fault is not observed here. Note the offset of the fan delta in the bathymetry dataset. Location of landslide/slump features north of Emerald Bay is also shown.

(Figs. 4&10). The north-facing slopes on General–Meeks and McKinney–General moraines have well developed recessional moraines that are preserved on the steep, north-facing slopes and are linear in form. Older bedrock faulting may be present beneath the moraines, but faulting of the character observed from the southern portion of the basin, and in other sedimentary areas, is not observed here. It should be noted that the apparent northern segment boundary of the RS or change in relief across the scarp is a consequence of the McKinney Bay slide (Fig. 2), in contrast to the nearly 1.5 km stepover between the FLS and RS of the WTDPF.

Dollar Point Segment

North of McKinney Bay, the WTDPF follows submerged topography, this time through a shallow, offshore shoal (Figs. 5&11). In this location, the topography has both a more gentle and blunt slope; instead of forming a steep wall as it does to the south, the scarp is less strongly developed to the north. A secondary splay just to the east near this bench may

help distribute some of the total slip, although due to the short length of this structure, it is likely minor in comparison to the transfer of slip to the other north-easterly faults, including the Stateline–North Tahoe fault and Incline Village fault.

The DPS scarp is also observed onshore in the LiDAR data. At Dollar Point, the DPS splays into at least three poorly defined, west-northwest and north–northwest trending fault traces (Fig. 2). The fault scarps, measured both from the LiDAR and from field investigation, are approximately 15 to 20 m high (likely in Younger or Older Tahoe till based on weathering) for the west-northwest trending structure and significantly higher (~30 m or more, some bedrock) for the more northerly oriented fault scarps. The high offset for both scarps suggests that they record a multitude of rupture events (Fig. 11). The more northerly oriented features are formed in more competent rock and may integrate a much longer span of time in relation to many other scarps observed within the basin that are likely reset by either Tahoe- or Tioga-aged glaciation.

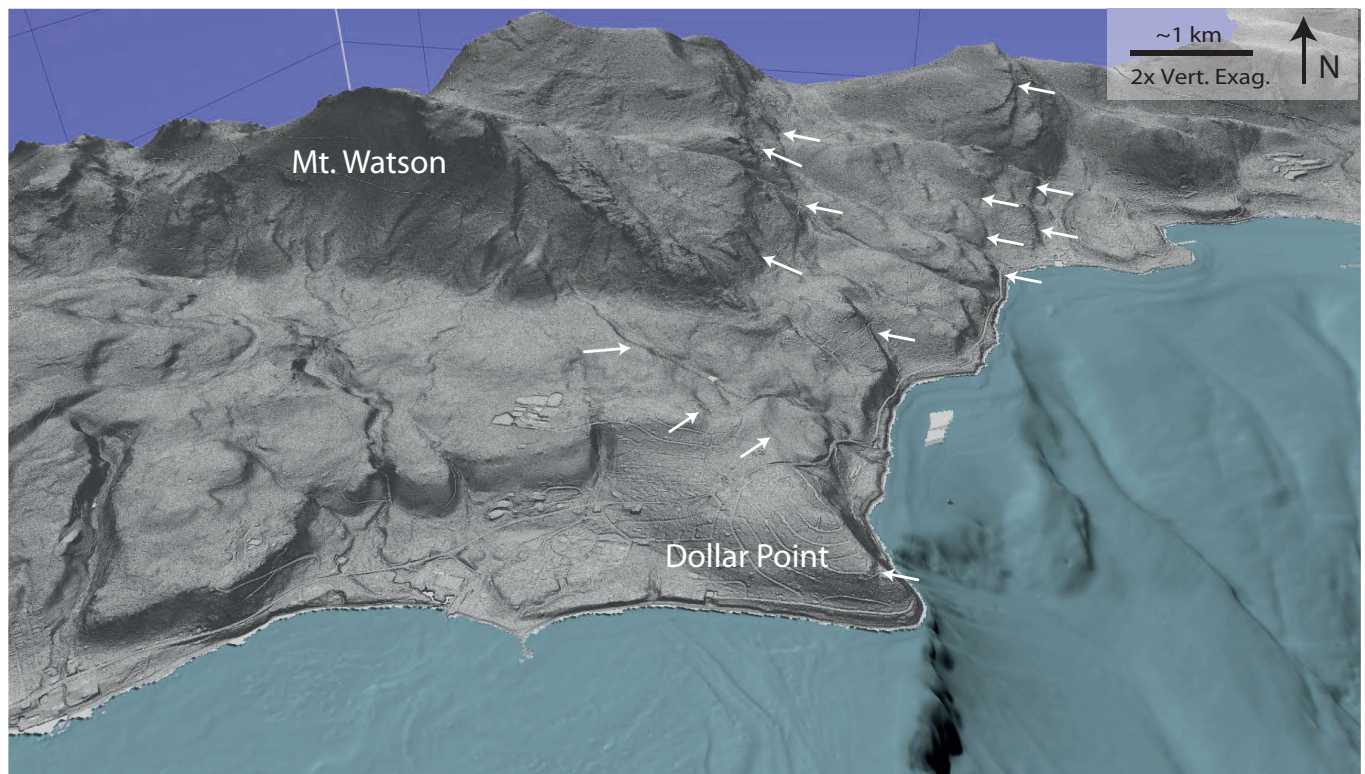


Figure 11. A slope-shade bare earth LiDAR model of the Tahoe basin near Dollar Point is shown. At this location, the orientation of the West Tahoe–Dollar Point fault changes from a north-northwest trend to a predominantly west-northwest trend. The fault appears to be dying out northwest of Dollar Point, although it may be influenced by the Polaris Fault zone farther to the northwest.

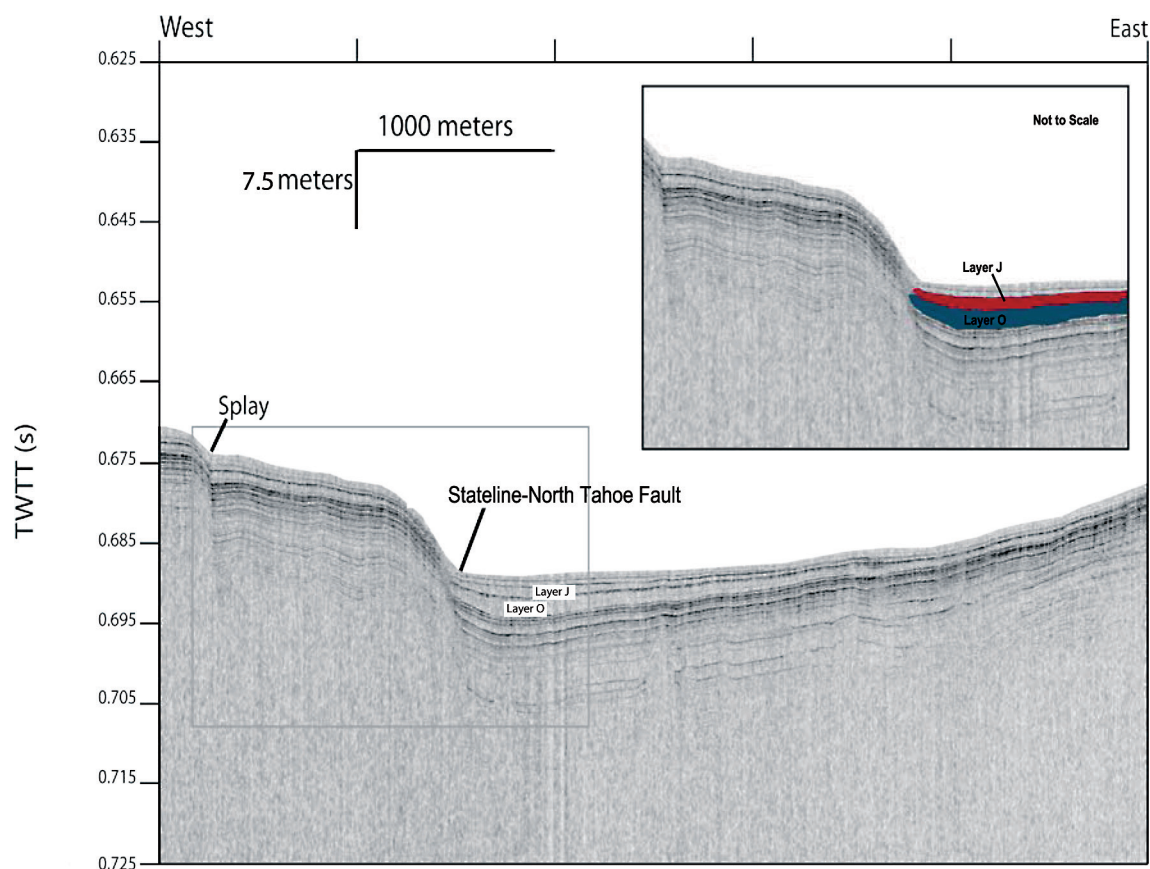


Figure 12. CHIRP profile (Day 3 Line 8, Figure 2) is shown, highlighting a west–east traverse across the Stateline–North Tahoe fault and an associated synthetic splay to the west. The alternating white and dark layers represent various sediment deposits. The thick acoustically transparent turbidite layer, labeled O, was deposited approximately 11,500 years BP and is likely the result of a major rupture on either the Stateline–North Tahoe fault, West Tahoe–Dollar Point fault, or both. Layer J appears to have been deposited at 7,800 years B.P., with the notion that both the West Tahoe–Dollar Point fault and Stateline–North Tahoe fault may be synchronized producing indistinguishable turbidite sequences. (inset) Turbidite layers J and O are colored magenta (J) and blue (O) for reference.

Scarp heights along the west-northwest trending structure decrease to the northwest and we do not observe a strongly developed main fault trace in the LiDAR data. This type of geometry is characteristic of what occurs near the ends of a fault as strike orientation can change dramatically. However, the orientation of the north-northwestward trending DPS scarps is spatially correlative to the newly identified Polaris Fault zone (Hunter et al., 2011). Therefore, the possibility exists that the DPS of the WTDPF is transferring slip into the Polaris fault zone, highlighting a transition from a mostly normal fault system, into one that is more characterized by right-lateral strike slip faulting.

Stateline–North Tahoe fault

The 1998 bathymetry map of Gardner et al. (2000) captures most of the Stateline–North Tahoe fault (SLNTF) structure, although our 2011 CHIRP imagery improves mapping of both the northern and southern extent (Figs. 2, 12&13). This is especially true to the south, where the fault scarp is subdued due to parity between slip rate and sediment deposition, which is observed in CHIRP profiles. These additional data confirm that the SLNTF is an east-dipping normal fault with up to ~24 meters of offset vertical separation across the McKinney Bay slide complex. Sediments on the hanging wall (east) side of the fault gradually tilt and thicken

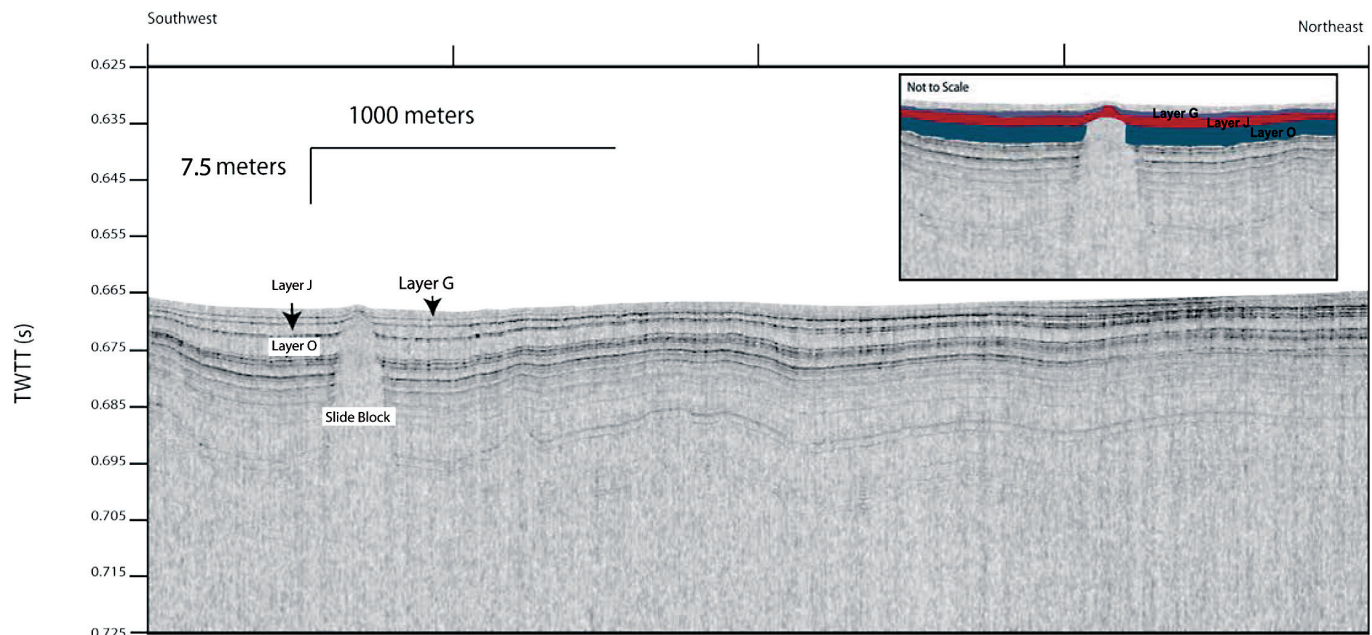


Figure 13. CHIRP profile (Day 3 Line 9, Figure 2) oriented southwest to northeast is shown. The alternating white and dark layers represent various sedimentation deposits. Turbidite deposits following the nomenclature of Smith et al. (2103) are labeled. A thinner Layer G deposited approximately 5,300 years B.P. is thought to be associated with an earthquake rupture on the West Tahoe–Dollar Point fault (Maloney et al., 2013). Acoustically transparent feature imaged along the southwest portion is interpreted as a slide block associated with the McKinney Bay slide. (inset) Turbidite layers J and O are colored magenta (J) and blue (O) for reference.

towards the fault, which is a typical geometry of growth faulting; on the footwall (west) side of the fault, the sediments thin considerably just west of the fault scarp. A representative CHIRP profile across the SLNTF highlights shallow fault structure centered at a small stepover (Fig. 12). The alternating light and dark acoustic layers are typically indicative of turbidite/debris deposition (Smith et al., 2013). The transparent layers (up to 2.2 m thick) with little stratigraphic layering are debris flows, likely sourced from the nearby Crystal Bay escarpment (Smith et al., 2013). These layers are quite continuous along the strike of the fault/escarpment as shown in Figure 13. The fault itself dips east with a maximum scarp height in this region of approximately 12 m. The dying strand at the stepover, located approximately 200 meters to the west of the main trace of the SLNTF, is also observed with a smaller, 3–4 m scarp (Fig. 12).

Near Crystal Bay on the north end of Lake Tahoe, the trace of the SLNTF reaches the shoreline, though is not easily traced outside of the lake. Fault-related features, such as a prominent scarp,

have not been confidently identified through either the LiDAR data nor field exploration and mapping. The regional published geologic map (Saucedo, 2005) indicates that the surficial geologic deposits in this area are Quaternary unnamed gravels, sand and alluvium of Pleistocene age. It is possible that the fault trace in this area is present, though not observed in the sedimentary deposits; this may be due to unconsolidated sediments that do not retain fault-related geomorphological features, or to stream related erosion that may be reworking the landscape. It is also possible that the fault does not extend north of the lakeshore and that that slip that was once accommodated by a longer SLNTF, is now taken up by the IVF to the east.

Incline Village Fault

The Incline Village fault (IVF) is traced in Lake Tahoe along a prominent submarine ridge from the shoreline to full water depth, and is roughly parallel to the Stateline–North Tahoe fault (SLNTF, Fig. 2). The fault extends north of the lakeshore, parallel to the Mt. Rose highway corridor, to slightly north of the manmade Incline Lake. In Lake Tahoe,

CHIRP profiles indicate the main fault trace is normal, down-to-the-east; some synthetic east dipping faults are observed in the vicinity of a small stepover in fault structure near the shoreline. Dingler et al. (2009) observed an offset boulder layer that provides evidence for ~14 meters of vertical deformation across the fault since the Tahoe glaciation. Paleoseismic trenching onshore indicates the most recent rupture of this fault occurred ~500 years B.P. (Seitz et al., 2005; Seitz et al., this issue).

The nearshore and onshore component of the IVF is a north-northeast striking normal fault that continues northward through the community of Incline Village before terminating near the base of Relay Peak, just to the northwest of Incline Lake (Fig. 14). The fault scarp is clearly visible throughout the community, where the fault emerges near the lake, crosses Lakeshore Blvd, and continues parallel to South/North Blvd, where it is clearly visible behind the former Incline Village Elementary School. At this point, the fault scarp is approximately 8 meters in height, and offsets beach deposits mantled by some glacial till.

North of Incline Village, the fault continues along the south side of a subsidiary flank of Relay Peak. The fault scarp is clearly evident on the ground

in this location. Near the vicinity of Incline Lake (Figs. 6&14), the fault jogs west and climbs Relay Peak, away from Incline Lake. Near this location, the scarp is approximately 2-4 meters high, and offsets likely Tioga-aged deposits. Again, the fault can be traced on the ground in this location. Near Incline Lake, there is significant historical anthropological disruption of the ground surface. This disruption includes ground terraces and cuts, which are evidence of road building and dam development, and makes tracing the fault more difficult on the ground; nevertheless, the fault is clearly evident in the LiDAR data.

Discussion:

Fault Density and Architecture

The primary purpose of our study was two-fold: (1) to identify the location of active faults in the Tahoe basin, recorded within late Pleistocene– and Holocene–aged deposits, using the latest arsenal of sophisticated mapping tools (i.e., LiDAR, seismic CHIRP profiling and multibeam sonar); (2) to find potential piercing points that may give constraints on any right-lateral (or left-lateral) motion on the major normal faults within the basin, and/or newly discovered faults. The application of airborne



Figure 14. A slope-shade bare earth LiDAR model highlighting the Incline Village fault is shown. The southern terminus of this fault extends some 10 kilometers into the lake. Onshore, the Incline Village fault traverses through neighborhoods before trending north-northeastward up the Mt. Rose Highway corridor before dying out to the west of the former Incline Lake dam abutment.

LiDAR to the Tahoe basin was a critical step in helping to resolve the disparity in fault architecture as reported from terrestrial mapping (Schweickert et al., 2004) and within lakes using sub-bottom sonar mapping techniques (e.g., Dingler et al., 2009; Brothers et al., 2009). At first glance, the lake studies provide what appears to be a relatively simple architecture, with a system of three en-echelon, right-stepping, down-to-the-east normal faults, and little evidence for a multitude of associated fault structures. This appears to be in conflict with the Schweickert et al. (2000; 2004) fault map, and further refinement by Howle et al. (2012), which used an earlier Army Corps of Engineers LiDAR survey that show a plethora of fault structures on land (Fig. 1). These terrestrial fault maps disagree (in terms of density) with the fault maps derived from offshore multibeam bathymetry and seismic CHIRP data. The most notable difference is along the west shore of Lake Tahoe, where the Tahoe-Sierra frontal fault zone has been mapped as a series of four closely spaced faults with a NW-SE orientation near Meeks Bay (e.g., Howle et al., 2012). Integrated separation across this zone is reported to be nearly 1.5 mm/yr of down-to-the east normal motion, which is more than twice the observed WTDPF rate (Dingler et al., 2009). This region of the basin is characterized by three to four prominent lateral moraines from glaciers sourced in the Desolation Wilderness, and are composed of pre Tahoe-, Tahoe- and Tioga-aged material (Howle et al., 2012).

The most striking observation from the 2010 Watershed Sciences bare-earth LiDAR data is the high-resolution imaging of the terrestrial portions of the WTDPF and IVF active fault scarps. Slope-shade maps derived from digital elevation models (DEM) clearly highlight fault scarps in a variety of terrains that include flat lying regions, steep hillsides, and across lateral moraines. The FLS of the WTDPF provides a template for fault identification in other regions of the basin, given the multitude of landforms that are offset by this segment. Although the WTDPF fault trace south of Fallen Leaf Lake appears rather straightforward in terms of structural complexity, aside from a nearly one-half kilometer stepover near Angora

Lakes, it also has a curious behavior of climbing up the steep hillside near Earthquake Lake. This observation implies some level of reorganization of slip as the fault abandoned its position at the base of the range front. In contrast, north of Fallen Leaf Lake, the FLS of the WTDPF appears to break into two separate strands, one maintaining its position near the edge of the range front, the other outboard toward Lake Tahoe, where the LiDAR data suggests that it enters the lake west of Baldwin Beach. This level of fault complexity may play an important role in the transfer of strain across the relatively large 1.5 km right-stepover between the FLS and RS of the WTDPF.

Onshore north of Emerald Bay, in the region of Rubicon and Meeks Bay, through-going structures similar to those found along the FLS of the WTDPF are lacking. There is some hint of what appears to be a fault-like structure emerging from the central portion Emerald Bay heading to the north, but careful analysis suggests it may owe its existence to mass-wasting of material downslope (Fig. 15). North of these landslide features, the moraines near Meeks Bay appear to be devoid of any topographic features that show linearity and/or continuity from moraine crest to moraine crest. The lead and second authors have walked the moraine crests both north and south of Emerald Bay to understand the features mapped by both Schweickert et al. (2004) and Howle et al. (2012). Unlike faulted moraines along the FLS of the WTDPF, the slopes of the moraines in this area appear devoid of any obvious fault scarps. If through-going structures along the Tahoe-Sierra frontal fault system exist as purported by Howle et al. (2012), then it is difficult to explain why they were not obviously imaged in the LiDAR data, given the clear imaging of ruptures along the FLS of the WTDPF.

The most complicating factor along the northern stretch (Dollar Point segment) of the WTDPF is that several splays integrate across more competent material (e.g., in some cases bedrock), and thus, may record a longer period of slip than those regions that have been “reset” by Tahoe and Tioga glaciation. The observed horsetailing of fault structure, including dramatic changes in strike, are consistent with terminations of normal fault systems

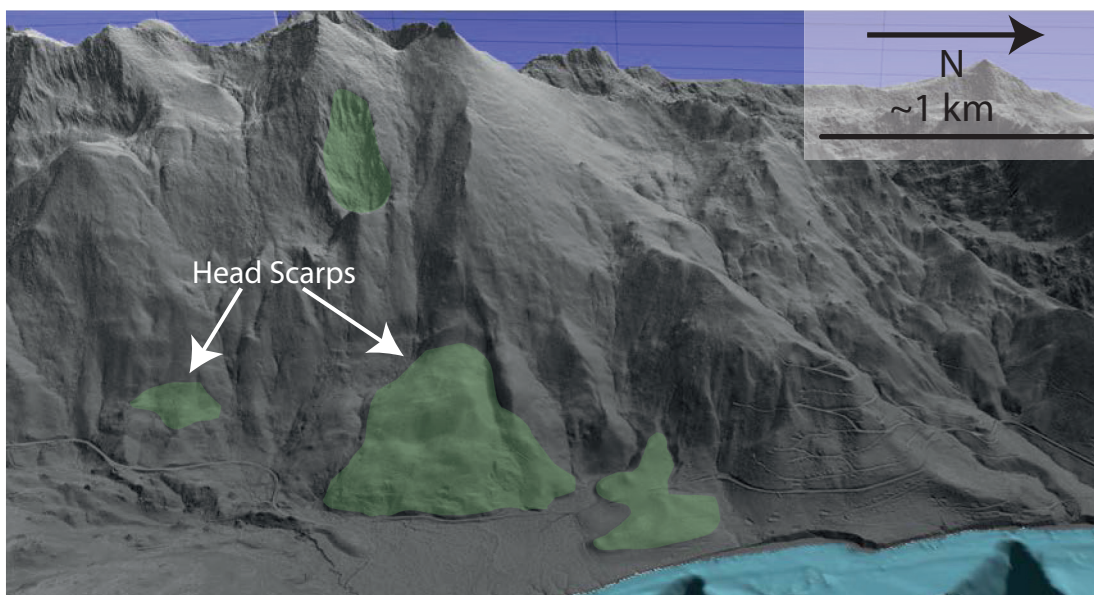


Figure 15. A slope-shade bare earth LiDAR image shows features interpreted to be landslides (shown in green) and their associated head scarps just north of Emerald Bay. The terrain in this area is highly susceptible to landslides.

(Faulds et al., 2011). Kinematically, changes in fault location as well as the progressive opening of the basin may be related to a slight counter-clockwise (CCW) rotation or pivot along the eastern edge of the Sierra Nevada microplate. This rotation would drive the basins to open northward through time as observed in the overall morphology of the Tahoe basin. This change in microplate kinematics may be relatively recent, based on evidence from the geomorphology of the SLNTF. The scarp height diminishes abruptly where it steps onshore at Crystal Bay. South of the 400 m scarp, on the floor in Lake Tahoe, scarp height varies from on-order 10 m in height to barely visible due to either diminished slip and/or sedimentation rate outpacing accommodation. One can invoke a long-term history of diminished slip along the southern extent of the SLNTF that has greatly muted the fault scarp height, or perhaps a model where recent propagation of the SLNTF toward the south where it dies mid-lake, helps to “open” the basin northward. In this model, the DPS of the WTDPF has diminishing slip over this time period, as more and more slip has been transferred over to the southward propagating SLNTF.

Tahoe–Sierra Frontal Fault Zone

Research published in the early 2000’s by Howle (2000) and Schweickert et al. (2004) commented that the NW-SE-oriented Tahoe-Sierra frontal fault system is a “complex zone which includes numerous subparallel, steeply east-dipping faults with apparent east-side-down normal displacement” and “carefully documented sinistral oblique displacements along several faults cutting glacial moraines along Meeks Creek southwest of Meeks Bay.” Recently, a subset of these authors published an update to their previous work (Howle et al., 2012) that provides more detailed evidence (through the use of 2008 Army Corps airborne LiDAR) of normal motion (1.5 ± 0.4 mm/yr) along the frontal fault system, but there wasn’t any discussion of sinistral (or dextral) motion along this fault zone. Instead, Howle et al. (2012) highlighted the tectonic geomorphology of faulted lateral/medial moraines to include side-slope troughs, back-titled moraine crests, triangular-faceted moraine scarps, and extensional fault-propagation folds in lateral/medial moraines (or “blind normal faults”). Their approach was to use indirect indicators of fault motion (e.g., back tilting of moraine crests) if obvious geomorphic features such as scarps were lacking. South of Emerald Bay, faults mapped by

Howle et al. (2012) are in general agreement with this study regarding location, as scarps are prominent, continuous features, cross lateral/medial moraines, and are imaged either atop the crest and/or on the sides of the steepened moraines.

North of Emerald Bay, there remains a strong disagreement on the existence of the Tahoe–Sierra frontal fault system, which provides two dramatically different views on the fault architecture of the Tahoe basin: Howle et al. (2012) argue that the Tahoe–Sierra frontal fault system connects with our FLS segment of the WTDPF to provide a longer frontal fault system at the expense of a shortened WTDPF. This disagreement has profound implications on fault length, maximum earthquake magnitude, and time evolution of basin formation. Our research suggests the FLS of the WTDPF steps into the lake some 1.5 km northeast, linking up with the RS of the WTPDF; this stepover zone is made somewhat more complex by the identification of a second active strand just north of Fallen Leaf Lake that trends roughly northwest to north, moving offshore just west of Baldwin Beach. Our preferred model keeps slip-rates somewhat in check along the entire 55-km-long WTDPF, from the FLS to the DPS, with vertical rates ranging somewhere near 0.4–0.8 mm/yr (Dingler et al., 2009; Brothers et al., 2009). The Howle et al. (2012) model has 2 times greater vertical slip across the frontal fault system than observed on the WTDPF; this observation is at odds with basin morphology in that the WTDPF is the basin-bounding fault system responsible for much of the accommodation that formed the lake. Thus, for the Howle et al. (2012) model to be valid, it would require the frontal fault system to be a nascent one, otherwise the shoreline of yet a deeper lake would be shifted to the west coincident with a long term normal faulting history along the Tahoe–Sierra frontal fault system. Also, within a larger Tahoe–Sierra frontal fault system, slip-rates would nearly triple north of Emerald Bay, and yet fault signatures across the glacial moraines, as manifested by scarps, are much more subdued.

The use of indirect evidence for mapping faults across moraines is not without merit. For example, a well-exposed fault scarp near the Angora Lakes parking lot is located within a 35-m-deep

saddle, or depression, that cuts through the lateral moraine that bounds Fallen Leaf Lake to the west. Assuming a Younger Tahoe age of approximately 70 ka (Howle et al., 2012) and a slip-rate of 0.5 mm/year (within the range reported by Brothers et al. (2009) at Fallen Leaf Lake), then one can roughly calculate some level of parity between these observations. Maloney et al. (2013) mapped the FLS of the WTDPF transitioning through the southern third of Cascade Lake, where it begins to horsetail into a handful of splays upon exiting the western shoreline. To the north, the fault moves westward towards Emerald Bay, possibly dying out, but not before contributing to a complex 25-m notch in the medial moraine (likely modified through erosion). Although the fault scarp here is not as clean as seen near Angora Lakes, the dramatic expression of the scarp plunging into Cascade Lake from the east, combined with CHIRP imagery within Cascade Lake, provides some level of confidence that the fault has interacted with the medial moraine that separates Cascade Lake and Emerald Bay to the west.

It is clear that not all notches, changes in slope, and other indirect structures observed within moraines require faulting to produce the range of geomorphologic expressions observed in glacial terrains world-wide. If more direct indicators for fault movement are missing, or are at least ambiguous, how does one determine whether the feature in question is due to faulting, or just the imperfect construction of a moraine, further modified through time by erosion and/or slumping? If these features are due to coherent faulting, one would expect that they might be continuous from ridge crest to ridge crest with some level of linearity. Along this trend, a subsection of the fault might have a well-formed scarp that would aid in its identification. Absent linearity and any noticeable subsections containing an unambiguous scarp, interpretation becomes much more difficult. This can be made even more difficult by the presence of landslides that may produce scarps sourced through the process of mass wasting.

As previously mentioned, our interpretations diverge with previous work north of Emerald Bay as one approaches the moraines that are found near

Meeks Bay. Howle et al. (2012) identify a fault scarp, identified as the Rubicon Peak fault zone, emerging near the center of Emerald Bay, then wrapping around the range front. We also observe a system of scarps that extends some 4 km north of Emerald Bay, but a 1.5-kilometer-wide section may provide clues to their origin. The central piece is arcuate in shape and has many of the characteristics of slope failure, such as a noticeable head scarp, U-shaped scars, and slumps. Other examples of slides are observed both above this feature, and actually within the slide itself. There are also countless examples of slope failure observed in the LiDAR data between Emerald Bay and McKinney Bay, including a handful of large slides near Ellis Peak. Our interpretation is that the Rubicon Peak fault zone is more likely associated with mass wasting, not movement on a fault. Moving north, there are several prominent lateral and medial moraines near Meeks Bay, including Meeks Creek, General–Meeks, McKinney–General and McKinney moraines (after Howle et al., 2012). Slopes of this moraine complex do not perfectly grade toward the lake, and notches and “back-tilting” of the moraine crest, in several places are highlighted by Howle et al. (2012). The largest of the recognized facets is on-order of 25 m in height (Fig. 16). There is also some evidence for dextral offset (or apparent offset) of a likely Tioga-aged ridge crest along the General–Meeks moraine at the location of one of the largest facets (Fig. 4), but it is difficult to extrapolate this feature, at least in a right-lateral sense, to either Meeks Creek or McKinney–General moraines. This lack of continuity gives pause with regards to any sustained fault trend; in the Howle et al. (2012) model, the largest facets do not connect from moraine to moraine, causing significant swings in slip-rates over distances less than 2 km. Instead, some form of linearity is maintained at the expense of consistency of slip-rate over short distances. Thus, the only other potential forms of continuity would be the facets and breaks in slopes that might reveal a more continuous system below. Again, several facets are 10s of meters in height that would require (locally) an approximate 0.35 mm/yr vertical slip-rate if offsetting Younger Tahoe moraines as postulated by Howle et al. (2012). Summed across

several notches down the ridge crest, this provides an integrated vertical separation that is about 1.5 mm/yr. If the older moraines have been misidentified and are of Older Tahoe age, then slip-rates would be nearly halved. If the offset facets are indeed Younger Tahoe-aged, and the recessional moraines are Tioga-aged, then the side-wall linear ridges of the recessional moraines should have about one-fifth the accrued displacement relative to the Tahoe-aged features—or about 5 meters (Fig. 16). And yet, these linear features do not appear to show that degree of deformation within the LiDAR dataset; at best there’s a few meters of chatter along these linear features. This observation decreases confidence that these indirect indicators of slip are a useful proxy for fault slip in this particular area.

The moraines of Meeks Bay, however, do exhibit some curious behavior. While slip-rate estimates do not seem consistent when comparing Tahoe- and Tioga-related features, nonetheless there are several identifiable scarps across this complex. Mass wasting is common to the Tahoe basin, as evidenced by submarine slide deposits (Smith et al., 2013; Maloney et al., 2013), and the McKinney Bay landslide (Gardner et al., 2000), which exemplifies an extreme geologic event. The quadrant extending from Emerald Bay to McKinney Bay appears very prone to landslides, and one can obviously extend this northward where remnants of the McKinney Bay slide are sitting at the bottom of the lake. One possibility that would allow Tahoe-aged features to be offset, while Tioga-aged features remain intact, would be a large landslide, potentially associated with the McKinney Bay failure, where a southern sliver of the failure lurched forward, but only partially failed. That said, there appears to be a chaotic mixture of offsets on inferred Tahoe- and Tioga-aged moraines, making it difficult to piece together a coherent history of either slip or sliding.

Stateline–North Tahoe Fault and Synchronicity of Rupture

Analysis of CHIRP data collected during the summer of 2011 indicates that the SLNTF extends farther south than previously mapped. A map showing the trace of the SLNTF as determined from CHIRP profiling is shown in Figure 2. Additional profiling

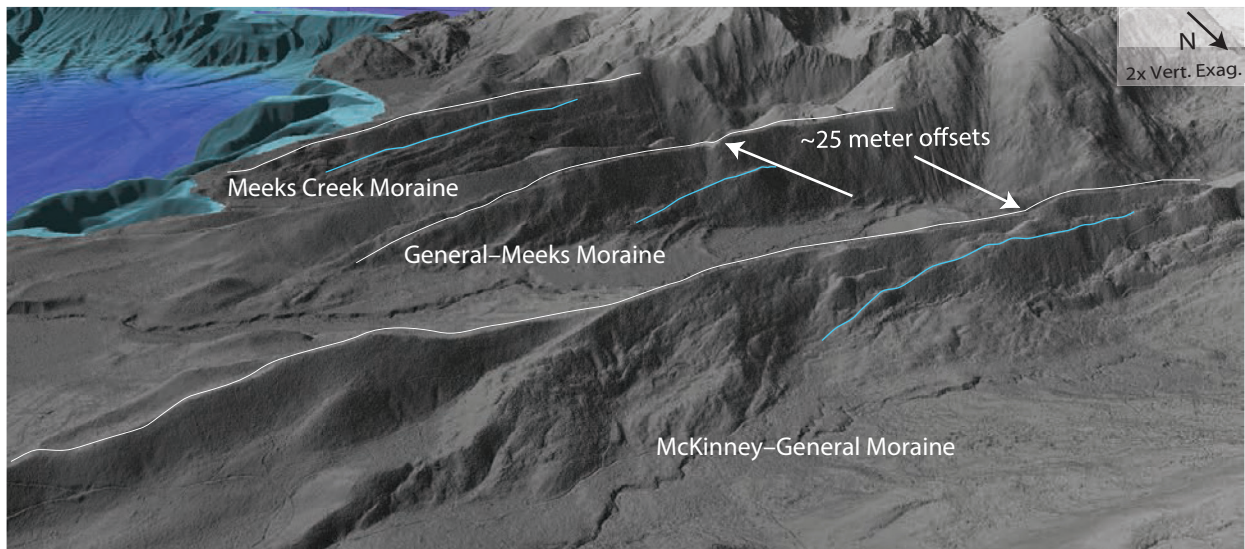


Figure 16. A slope shade bare earth LiDAR image of the Meeks Bay moraine complex is shown. White lines represent the moraine crests and cyan represents other linear features (recessional) on the north faces of the moraines. Notches observed along the moraine crests are measured, though similar or scaled offsets (through time) are not easily observed within other younger, linear features along the sides of the moraines. Linear continuity between the notches or across all moraines is not readily observed, nor is there evidence for faulting on the slopes or valleys between the moraines.

beyond the southern terminus of the mapped fault reveals that the SLNTF appears to step over towards the WTDPF; some evidence for discontinuous offsets of the McKinney Bay slide is observed in our profiles in this region. Local thickening of debris deposits near these steep faces, however, highlights that while there is ambiguity in terms of which fault produced the necessary ground motion to trigger the slide, there is more confidence in determining the source of the debris layer itself. The thick, non-reflective layers shown in Figures 12&13 (see red and blue layers) are landslide deposits, and likely sourced from the steep Crystal Bay escarpment. These debris layers grade into turbidite layers and are likely triggered by past earthquakes (Smith et al., 2013).

Maloney et al. (2013) and Smith et al. (2013) have studied landslide and turbidite deposits as a proxy for recent movement on Tahoe basin faults. Their research in Lake Tahoe (Smith et al., 2013) and moraine-bounded lakes south of Lake Tahoe (Maloney et al., 2013) indicate four temporally discrete, synchronous landslide events in Tahoe basin lakes that are likely the result of earthquakes on the WTDPF. Evidence for the concurrent timing

of fault rupture and landslide events is discussed in Maloney et al. (2013). The Most Recent Event (MRE) slide in Fallen Leaf Lake (Brothers et al., 2009; Maloney et al., 2013) infills accommodation created by the MRE earthquake at approximately 4.5 ka. This, along with sedimentological relationships between the MRE slide directly overlying the MRE stratigraphic horizon, suggest earthquake triggering of this particular landslide.

According to their studies, four landslide deposits can be correlated between Fallen Leaf Lake, Cascade Lake, Emerald Bay and Lake Tahoe, which suggest at least four earthquake events. Maloney et al. (2013) classifies these events as the ~11.5 ka event, ~8 ka event, MRE event on the RS (5.6 ka), and MRE on the FLS (~4.5 ka). Although other slide and turbidite deposits are present in both Lake Tahoe and the moraine-bounded lakes to the south, these four deposits provide the best evidence for movement on the WTDPF. Figure 13 shows a CHIRP profile paralleling the Crystal Bay escarpment; debris deposits lacking reflectivity are clearly visible as thick (meter-scale) deposits interbedded with thinner lacustrine deposits. Extrapolation of dated cores 20 and 21 (Smith et al., 2013) identify the two largest slides to

be temporally equivalent to Slides O and J in the central and southern reaches of Lake Tahoe. These slides have maximum thicknesses of 220 cm and 130 cm for deposits O and J (Fig. 12), respectively.

Although rupture on the SLNTF is observed in the CHIRP data as offset beds, the timing of rupture events is not well constrained as slip on this fault outpaces sedimentation to infill accommodation. This relationship prevents an easy identification of event chronology in the CHIRP data (Brothers et al., 2009). It is likely that debris/turbidite deposits in Lake Tahoe found near the Crystal Bay escarpment are sourced from earthquakes on the SLNTF, instead of earthquakes on the WTDPF, although this latter option cannot be dismissed. Based on our new data, we recognize that turbidite Deposits J and O (definitions from Smith et al., 2013; Maloney et al., 2013) have enhanced thicknesses near the northern section of the SLNTF, suggesting a local source (i.e., Crystal Bay escarpment). More importantly, debris deposits sourced near the SLNTF appear to have a similar chronology to those observed along the RS of the WTDPF. This suggests that both the WTDPF and SLNTF share the same or inseparable chronology of debris-related turbidite deposits. Perhaps Deposits O and J, observed as far south as the southern moraine-bounded lakes, are all related to rupture on the WTDPF. If true, then it is odd that the SLNTF does not have its own distinct chronology of rupture (at least within the temporal resolution afforded by CHIRP profiling and dating). Alternatively, both the WTDPF and SLNTF may rupture synchronously, thus providing little time for background sedimentation rates to effectively separate debris deposits in depth that are close in time.

In a discussion of rupture synchronicity, Scholz (2010) explains the timing similarities observed in both the Basin and Range province in Nevada and the Eastern California Shear Zone. His study area is especially fitting considering the Lake Tahoe basin is influenced by both of these systems. In his work, Scholz describes clusters of events and the properties of the faults that make them likely to exhibit synchronistic behavior. Typically, synchronicity occurs within systems of evenly

spaced, subparallel faults that have very similar slip rates. Additionally, each fault must be near the end of its rupture cycle so that the change in the stress caused by the first earthquake is enough to initiate a second earthquake on a nearby fault. Scholz (2010) found in his work that triggered earthquakes typically occur within 0.1 to 1.0 years after the triggering event, though this time may be slightly longer, depending on the system. He suggests it takes a very small stress drop, on the order of 0.1 to 0.01 MPa, to trigger an earthquake on an adjacent fault late in its inter-seismic period.

Based on previous work (Kent et al., 2005; Dingler et al., 2009), slip rates for the WTDPF and SLNTF are estimated to be similar, with a slip rate on the WTDPF of approximately 0.4 to 0.8 mm/yr and on the SLNTF of approximately 0.35 to 0.6 mm/yr. Because the slip rate on the IVF is much less at approximately 0.1 to 0.2 mm/yr, and its rupture timing does not appear to coincide with either the WTDPF or the SLNTF, it is not considered part of this potential sequence. The subparallel faults are approximately eight to ten kilometers apart, making them an ideal system for synchronized behavior. Since a historical record of rupture on these faults does not exist, and the spatial resolution of our data is insufficient to identify short time lapses (days to ~100 years) between events, it is unclear if these faults rupture as a cluster. Nevertheless, the size of debris flow Deposits O and J provide indirect evidence of large and possibly synchronous rupture.

Conclusions

Prior to the 2010 LiDAR survey, the fault complexity interpreted by previous workers on land appeared higher than that observed in Lake Tahoe. Previous work in Lake Tahoe (Brothers et al., 2009; Dingler et al., 2009) clearly showed evidence for relatively simple fault geometries within the deepest part of the basin. These results were inconsistent with work published by Schweickert et al. (2004) and Howle et al. (2012), who documented very complex fault geometries on land. We argue that the fault geometry on land is less complicated than previously thought and that it more consistent with the fault geometry imaged

within Lake Tahoe. The combined approach of this study clearly shows the locations of the major active faults in the Tahoe basin. Between the newly acquired LiDAR data and the addition of the new CHIRP and multibeam data, the normal faults have been mapped both onshore and within lakes.

Analysis of LiDAR data between Emerald Bay and Meeks Bay highlights the roles of glaciation, tectonics and mass wasting in the evolution of topography. Although the moraine crests of Meeks Bay show a degree of complexity, through-going structures are difficult to identify. While correlation of potential Tahoe-age triangular facets and back-tilted slopes from moraine crest to moraine crest is somewhat possible, Tioga-age recessional moraines preserved on the north slopes of these moraines do not show corresponding offsets (about 1/5th of the displacement), which is inconsistent with a fault-based origin. Instead, we speculate that some of these features may be related to mass movement associated with the McKinney Bay slide or other mass wasting events. The few candidate piercing points in the basin along faulted lateral moraines near Angora and Cascade lakes do not show progressive offset between Tioga- and Tahoe-aged features; instead, likely natural variability of geomorphic shape provide inconsistent offsets that are not consistent with any right lateral motion.

New CHIRP data crossing the full expanse of the SLNTF provide new clues into the total fault length, its dynamics through time, and the potential for synchronous ruptures between the largest two basin bounding faults. The SLNTF is longer than previously mapped, extending into mid-lake. The dramatic change in scarp height away from Crystal Bay would lead one to consider the possibility of a southward propagation (or growth) through time of the SLNTF, with deformation along the DPS of the WTDPF potentially dying away over this period. This evolution would help “open” basin geometry to the north, thereby contributing to left-lateral shear in the northern basin. Observed changes in the geometry of the FLS of the WTDPF also

highlight a very dynamic environment for fault reorganization. Lastly, locally-sourced large debris flows off of the Crystal Bay escarpment near the SLNTF have a chronology that is similar to the large slides sourced off of the Rubicon escarpment along the RS of the WTDPF. Given the slip rates of each fault and characteristic return time between ruptures, there exists the possibility that these systems may have experienced synchronous ruptures (decadal time-scale), highlighting a system that may be similar to that observed in the Central Nevada Seismic Belt in the 1950s.

Acknowledgements

We thank Shane Romsos at the Tahoe Regional Planning Agency (TRPA) for leading the efforts to collect the 2010 LiDAR dataset. The LiDAR campaign was successful in part due to the work of Ramon Arrowsmith (ASU) and Chris Crosby (UCSD) in contractor selection. This research was funded through USGS NEHRP grants G13AP00017 and 10HQA1000. This manuscript was greatly improved with reviews from Steve Wesnousky, Jeff Unruh and Tim McCrink.

REFERENCES

- Birkeland, P.W., 1963, Pleistocene volcanics and deformation of the Truckee area, north of Lake Tahoe, California, *Geol. Soc. America Bull.*, v. 74, p. 1453–1464.
- Blackwelder, E., 1933, Eastern slope of the Sierra Nevada, *16th Internat. Geological Cong., Guidebook 16*, p. 81–95.
- Bormann, J. M., 2013, New Insights into Strain Accumulation and Release in the Central and Northern Walker Lane, Pacific-North American Plate Boundary, California and Nevada, USA [Doctorate Dissertation]: University of Nevada, Reno, 150 p.
- Brothers, D. S., Kent, G. M., Driscoll, N. W., Smith, S. B., Karlin, R., Dingler, J. A., Harding, A. J., Seitz, G. G., and Babcock, J. M., 2009, New constraints on deformation, slip rate, and timing of the most recent earthquake on the West Tahoe-Dollar Point Fault, Lake Tahoe Basin, California: *Bulletin of the Seismological Society of America*, v. 99, no. 2A, p. 499–519.

- Busby, C. J., 2013, Birth of a Plate Boundary at ~12 Ma in the Ancestral Cascades Arc, and implications for transtensional rift development, Walker Lane belt, *Geol. Soc. Am. Bull.*, 9,(5) 14pp., doi:10.1130/GES00928.
- Cashman, P. H., and S. A. Fontaine, Strain partitioning in the northern Walker Lane, western Nevada and northeastern California, *Tectonophysics*, 326, 111–130, 2000.
- Dingler, J., Kent, G., Driscoll, N., Babcock, J., Harding, A., Seitz, G., Karlin, B., and Goldman, C., 2009, A high-resolution seismic CHIRP investigation of active normal faulting across Lake Tahoe basin, California-Nevada: Geological Society of America Bulletin, v. 121, no. 7-8, p. 1089–1107.
- Faulds, J. E., Hinz, J.H., Coolbaugh, M.F., Cashman, P.H., Kratt, C., Dering, G., Edwards, J., Mayhew, B., McLachlan, H., 2011, Assessment of Favorable Structural Settings of Geothermal Systems in the Great Basin, Western, USA, *GRC Transactions*, Vol. 35.
- Gardner, J. V., Mayer, L. A., and Hughs Clarke, J. E., 2000, Morphology and processes in Lake Tahoe (California-Nevada): Bulletin of the Geological Society of America, v. 112, no. 5, p. 736–746.
- Hammond, W. C., G. Blewitt, and Kreemer, C., 2011, Block modeling of crustal deformation of the northern Walker Lane and Basin and Range from GPS velocities: *J. Geophys. Res.*, 116, B04402, doi:10.1029/2010JB007817, p. 1–28.
- Howle, J.F., 2000, The Meeks Bay right lateral moraines and implications to late Pleistocene glaciations, Lake Tahoe elevations, neotectonics, and fault geometry, (abs.), *Abstr. Programs-Geol. Soc. Am.* 33, A67.
- Howle, J. F., G. W. Bawden, R. A. Schweickert, R. C. Finkel, L. E. Hunter, R. S. Rose and B. von Twisting, 2012, Airborne LiDAR analysis and geochronology of faulted glacial moraines in the Tahoe Sierra frontal fault zone reveal substantial seismic hazards in the Lake Tahoe region, California-Nevada, USA, *Bull. Geol. Soc. Am.*, doi. 10.1130/830598.1
- Hunter, L. E., J. F. Howle, R. S. Rose, and G. W. Bawden, 2011, LiDAR-assisted identification of an active fault near Truckee, California, *Bull. Seis. Soc. Am.*, 101, pp. 1162–1181.
- Hyne, N. J., Chelminski, P., Court, J. E., Gorsline, D. S., and Goldman, C. R., 1972, Quaternary History of Lake Tahoe, California-Nevada: Geological Society of America Bulletin, v. 83, no. 5, p. 1435–1448.
- Kent, G. M., Babcock, J. M., Driscoll, N. W., Harding, A. J., Dingler, J. A., Seitz, G. G., Gardner, J.V., Mayer, L. A., Goldman, C. R., Heyvaert, A. C., Richards, R. C., Karlin, R., Morgan, C.W., Gayes, P.T., and Owen, L.A., 2005, 60 k.y. record of extension across the western boundary of the Basin and Range province: Estimate of slip rates from offset shoreline terraces and a catastrophic slide beneath Lake Tahoe: *Geology*, v. 33, no. 5, p. 365–368.
- Lindgren, W., 1911, The Tertiary gravels of the Sierra Nevada of California: *U.S. Geol. Survey Prof. Paper 73*, p. 9–81.
- Maloney, J.M., Noble, P.J., Driscoll, N.W., Kent G.M., Smith, S.B., Schmauder, G.C., Babcock, J.M., Baskin, R.L., Karlin, R., Kell, A.M., Seitz, G.G., Kleppe, J.A., 2013, Paleoseismic history of the Fallen Leaf Segment of the West Tahoe-Dollar Point fault reconstructed from slide deposits in the Lake Tahoe Basin, California-Nevada, *Geosphere*, v. 9, no. 4, p. 1065–1090. doi: 10.1130/GES00877.1.
- Saucedo, G. J., Little, J. D., Watkins, S. E., Davis, J. R., Mascorro, M. T., Walker, V. D., and Ford, E. W., 2005, Geologic map of the Lake Tahoe Basin, California and Nevada: California Geological Survey, Regional Geologic Map No. 4, scale 1:100,000.
- Scholz, C.H., 2010, Large Earthquake Triggering, Clustering, and the Synchronization of Faults, *Bull. Seismol. Soc. Am.*, Vol. 100, No. 3, pp. 901–909.
- Schweickert, R. A., Lahren, M. M., Smith, K., and Karlin, R., 1999, Preliminary fault map of the Lake Tahoe basin, California and Nevada: *Seis. Res. Lett.*, v. 70, p. 306–312.
- Schweickert, R. A., Lahren, M. M., Smith, K. D., Howle, J. F., and Ichinose, G. A., 2004, Transtensional deformation in the Lake Tahoe region, California and Nevada, USA: *Tectonophysics*, v. 392, no. 1-4, p. 303–323.
- Seitz, G.G., Kent, G.M., Dingler, J.A., Karlin, B., and Turner, R., 2005, First paleoseismic results from the Lake Tahoe basin; evidence for three M 7 range earthquakes on the Incline Village fault: *Seismological Research Letters*, v. 76, p. 239–240.
- Smith, S. B., Karlin, R. E., Kent, G., Seitz, G., and Driscoll, N. W., 2013, Holocene Submarine Paleoseismology of Lake Tahoe: Geological Society of America Bulletin, v. 125, no. 1-2.
- Tahoe Regional Planning Agency (TRPA), 2010, Lake Tahoe Basin LiDAR: <http://dx.doi.org/10.5069/G9PN93H2> (October 2011).
- Unruh, J., Humphrey, J., and Barron, A., 2003, Transtensional model for the Sierra Nevada frontal fault system, eastern California: *Geology*, v. 31, no. 4, p. 327–330.

Watershed Sciences, 2010, LiDAR Remote Sensing, Lake Tahoe Watershed, prepared for the Tahoe Regional Planning Agency, January 31, 2011.

Wesnousky, S. G., Bormann, J. M., Kreemer, C., Hammond, W. C., and J. N. Brune (2012), Neotectonics, Geodesy, Seismic Hazard in the northern Walker Lane of Western North America: Thirty kilometers of crustal shear and no strike-slip? *Earth and Planetary Science Letters*, 329–330, 133–140

Graham M. Kent. Dr. Graham Kent, Director of the Nevada Seismological Laboratory, specializes in reflection seismology, mid-ocean ridge dynamics, tectonics of the Gulf of California–Walker Lane transtensional system, Southern California tectonics, development of underwater approaches to paleoseismology, and earth science-related high end visualization. Dr. Kent also works with instrumentation, including the development of a 100-instrument ocean-bottom seismograph pool (developed at Scripps, PI), and more recently, upgrading the microwave system in eastern California and Nevada to support digital delivery of “all hazards” to include: seismic, fire and extreme weather data types.

Gretchen C. Schmauder. Dr. Gretchen Schmauder is a former Ph.D. student at the University of Nevada, Reno (Nevada Seismological Laboratory), where she mapped fault structure at Lake Tahoe using a variety of techniques, including airborne LiDAR (Light Detection and Ranging) on land and underwater CHIRP sub-bottom profiling. She also used fault architecture and shallow velocity structure derived from REMI techniques to simulate ground motion from large damaging earthquakes in the Lake Tahoe Basin. She has since moved on to work at Geometrics Inc., where she is Customer Service Business Manager. Dr. Schmauder also has her license as a Professional Geologist.

Jillian Maloney is an assistant professor of geology at San Diego State University. Using both geologic and geophysical datasets, Maloney seeks to understand tectonic deformation and sediment processes along continental margins. Her research has focused on offshore neotectonics, paleoseismology, and landslide dynamics in tectonically active settings. Maloney has also conducted research on marine geohazards and sediment dispersal along passive margins.

Neal W. Driscoll. Dr. Neal Driscoll is a professor of geology and geophysics at Scripps Institution of Oceanography, University of California, San Diego. Driscoll’s primary interest is in tectonic deformation and the evolution of landscapes and seascapes. His work primarily focuses on the sediment record to understand the processes that shaped the earth.

Simply stated, stratigraphy is the tape recorder of Earth’s history. Nevertheless, the fidelity with which stratigraphy records the dynamic processes of sediment erosion, transport, accumulation, and preservation is still incompletely understood. Although these processes can be examined from many perspectives, Driscoll’s research has focused on unconformity generation and stratigraphic development in tectonically active settings and sediment input and dispersal along continental margins.

Annie Kell, Education Outreach Seismologist at the Nevada Seismological Laboratory, earned a Ph.D. in Geophysics in 2014. Her research focuses on seismic imaging of shallow crust in regions with active tectonics. Research areas include the Salton Sea, Pyramid Lake and Lake Tahoe. After experiencing a large magnitude earthquake in 2010, Annie became motivated to help educate Nevadans on earthquake hazards and safety preparation. The work allows her to continue to do research in interesting environments, but also to interact with emergency officials, school-aged children and the general public.

Kenneth D. Smith. Dr. Kenneth Smith, Assoc. Director of the Nevada Seismological Laboratory, specializes in earthquake studies of the Basin and Range of Nevada and eastern California. Dr. Smith manages the Nevada Seismic Network, which consists of ~150 seismograph stations and a regional microwave communications system (with primary support through the USGS and the State of Nevada); the Nevada Seismological Laboratory reports the locations and magnitudes of over 10,000 earthquakes per year in Nevada and eastern California. He was involved in seismic hazard studies and earthquake monitoring for the DOE’s Yucca Mountain Project (closed out in 2010). Dr. Smith manages the Nevada Seismological Laboratory’s role in the DOE’s ‘Source Physics Experiment’, being conducted by National Security Technologies on the Nevada National Security Site.

Robert L. Baskin. Dr. Rob Baskin is currently a Supervisory Hydrologist with the U.S. Geological Survey in Salt Lake City, Utah. Rob is involved in multiple studies; however, his primary research focuses on the integration of multiple technologies to establish the environmental framework that influences microbial bioherm occurrence and distribution in Great Salt Lake, Utah. He has conducted multiple collaborative studies on inland waterbodies with the Scripps Institution of Oceanography, University of California, San Diego, and the University of Nevada, Reno, including Great Salt Lake, the Salton Sea, Pyramid Lake, Lake Tahoe, Walker Lake and others. He was involved with early applications of thermal imagery in the study of groundwater inflow into lakes, and

recently completed his Doctoral dissertation at the University of Utah. He is also a registered professional geologist in the State of Utah.

Dr. Gordon Seitz is an Engineering Geologist at the California Geological Survey in Menlo Park, California. He is licensed in California as a Professional Geologist and Certified Engineering Geologist. He received his B.S. from San Diego State University,

and a Ph.D. from University of Oregon. His graduate research focused on paleoseismology. He completed a postdoctoral fellowship at Lawrence Livermore National Laboratory at the Center for Accelerator Mass Spectrometry, where he researched the dating of earthquakes using C-14 samples. He has participated in paleoseismic and earthquake investigations worldwide. He continues to work on developing offshore paleoseismic methodologies using Lake Tahoe as a laboratory.